EDITOR

Doç. Dr. Rukiye UZUN ARSLAN

Researches and Evaluations in the Field of

ELECTRICAL ELECTRONICS AND COMMUNICATION ENGINEERING

December 2024

İmtiyaz Sahibi / Yaşar Hız
Yayına Hazırlayan / Gece Kitaplığı
Birinci Basım / Aralık 2024 - Ankara
ISBN / 978-625-7177-81-8

Gece Kitaplığı
Kızılay Mah. Fevzi Çakmak 1. Sokak
Ümit Apt No: 22/A Çankaya/ANKARA
0312 384 80 40
www.gecekitapligi.com / gecekitapligi@gmail.com

Baskı & Cilt
Bizim Büro
Sertifika No: 42488

RESEARCHES AND EVALUATIONS

IN THE FIELD OF

ELECTRICAL-ELECTRONICS

AND

COMMUNICATION ENGINEERING

EDITOR

Doç. Dr. Rukiye UZUN ARSLAN

gece kitaplığı

CONTENTS

CHAPTER 1

ANALYSIS AND SIMULATION OF CLASSICAL AND MODIFIED QUADRATIC BOOST CONVERTERS

Asli Seyda IPEK[1], Naim Suleyman TING[2]

1 M.Sc. Student, Erzincan Binali Yildirim University, Institute of Science and Technology, Department of Electrical Electronics Engineering, a.seydaipek@outlook.com, ORCID: 0000-0001-6504-4125.

2 Prof. Dr., Erzincan Binali Yildirim University, Faculty of Engineering and Architecture, Department of Electrical Electronics Engineering, nsuleyman@erzincan.edu.tr, ORCID: 0000-0003-3743-0824.

1. INTRODUCTION

Energy is defined as the capacity to perform work of a system and is an indispensable component of modern life. Energy not only supplies individual needs, but also forms the foundation of many sectors such as industry, transportation and technology. For this reason, the demand for energy has continued to increase in every period of human history. This demand is reshaping the balance between non-renewable energy sources (fossil fuels, nuclear energy, etc.) and renewable energy sources (solar, wind, hydroelectricity, etc.). While the trend towards renewable energy sources is rapidly increasing today, non-renewable sources still compose of a large portion of energy consumption (Haegel et al., 2021). Non-renewable energy sources are energy types that are found in limited quantities in nature and cannot be replaced as they are consumed. Fossil fuels (coal, oil, natural gas, etc.) and nuclear energy are in this category. These sources have been used to ensure the energy needs of the modern world for many years. However, they pose serious problems in terms of sustainability due to their environmental impacts and limited reserves. Increasing environmental awareness and the advances in renewable energy technologies aim to reduce dependence on non-renewable energy sources. For this reason, accelerating the transition to renewable energy sources is critical to ensuring energy security and environmental sustainability in the future. Renewable energy sources are resources that are constantly renewed in nature and have no risk of depletion. Solar, wind, water, geothermal energy and biomass are the main examples of renewable energy sources. These sources are increasingly gaining importance due to their environmental friendliness and sustainable energy production. Therefore, increasing investments in renewable energy technologies is of great importance in order to build a livable world for future generations (Ogunrinde et al., 2018; Qazi et al., 2019).

Energy transformation is an important issue in renewable energy systems. While some sources provide AC energy, some sources provide DC energy. It is important that the energy provided by renewable energy sources is converted according to the AC or DC needs of the loads. In this context, one of the most widely used conversion techniques is DC-DC conversion. DC-DC converters used for this purpose are electronic circuits that convert one DC voltage level to another DC voltage level. In renewable energy systems, they are widely used to ensure the efficient operation of DC energy sources such as especially solar panels, fuel cells and batteries (Ting et al., 2023). DC-DC converters play a vital role in the efficient and stable management of energy production and storage processes. The low output voltage characteristics of renewable energy sources such as solar and fuel cells necessitate the use of these converters in industrial applications. For example; in solar panels, the output voltage changes continuously depending on the sunlight intensity and temperature. Similarly, the energy produced in wind turbines can fluctuate according to the wind speed. Most renewable energy sources, such as the examples given above, produce variable voltage and current depending on environmental conditions. DC-DC converters adjust these variable voltages to a fixed level that the load needs. These converters also provide efficiency optimization. Especially in solar energy systems, DC-DC converters can be operated with maximum power point tracking (MPPT) algorithms to obtain maximum efficiency from the energy source at the maximum power point. While solar panels generally produce output voltage between 18-48V, the batteries operate with fixed voltages such as 12V, 24V, 48V. DC-DC converters provide a balance between energy production and consumption by converting these different voltage levels to the required voltage level.

Modern converters recommended in the literature generally operate with an efficiency higher than 90%, which makes it possible to obtain maximum benefit from renewable energy sources (Lakshmi and Hemamalini, 2018). One of the most commonly used DC-DC converter type is the boost converter. Boost DC-DC converters are electronic circuits that convert the input voltage to a higher output voltage. These converters are used to increase the low voltage produced to a suitable voltage level for energy storage systems or loads in renewable energy systems such as especially solar panels, fuel cells, batteries. Solar panels and fuel cells generally produce low DC voltage (12V-48V). This voltage is not sufficient for inverters or grid connection. The voltage levels used for battery charging in electric vehicle charging stations are high (300V-400V). However, the voltage level of the batteries may decrease during discharge. For these reasons, the boost DC-DC converters used increase these low and variable voltage levels to a high level, ensuring the harmonious and efficient operation of the system (Lee and Do, 2019).

In the conventional boost converter, a voltage twice the input voltage can be obtained at the output at 50% duty cycle. Nowadays, the high-gain DC-DC converter topologies (Singh et al., 2022; Yang et al., 2009) where higher output voltage values can be obtained at the same duty cycle have been presented in the literature. The most well-known types of these topologies are interleaved, cascaded and quadratic DC-DC converters. The voltage gain in the interleaved DC-DC boost topology is the same as a conventional boost converter. The most important feature of this converter is that the input current ripple is lower (Ting et al., 2017). The interleaved structure distributes the load between multiple phases, allowing each phase to carry lower current. Synchronous operation of parallel phases reduces the switching and conduction power losses. This structure provides increased efficiency, especially in high powered applications. Cascade DC-DC boost converters are obtained by connecting multiple DC-DC boost converters in series. Multiple DC-DC boost converters are connected in a row, and each converter prepares the voltage level for the next stage. In the first stage, the low input voltage is converted to an intermediate voltage level. The voltage at the intermediate level is increased to the final output level by the second converter. The cascade boost DC-DC converter, which is the combination of two or more boost converters, is the simplest method to obtain a higher voltage conversion gain than the conventional boost converter. Cascade structures provide a very high voltage conversion ratio by using smaller conversion ratios at each stage (Yang et al., 2023). In briefly, the cascade DC-DC boost converters offer the advantages of higher conversion ratios and modular design with compared to conventional DC-DC boost converters. While it is preferred especially in renewable energy systems and high-power applications, its disadvantages such as complex structure, cost, and reduced efficiency at each stage should be taken into consideration. In another structure, the classical quadratic boost converter (CQBC) present a voltage four times the input voltage at the output at 50% duty cycle unlike the conventional boost converter (Ahmad et al., 2021). Quadratic boost converter (QBC) is an effective and innovative solution for modern energy systems requiring high voltage conversion ratios. While it offers a higher conversion ratio than conventional boost converters, it provides a more compact and efficient performance with compared to cascade structures. It increases the life of the elements due to low current and voltage stresses with compared to interleaved converters. Although each converter type has its own advantages and areas of use, quadratic boost converters stand out especially in systems requiring high conversion ratios and minimizing energy losses. Many studies have been proposed about this topic in the literature and many different circuits have been designed using quadratic DC-DC boost converters (Tattiwong and Bunlaksananusorn, 2014; Naresh et al., 2025).

In this chapter, CQBC and high gain modified quadratic boost converter (MQBC) proposed in the literature are selected and their working principles are discussed in detail. In addition, the operating modes of these converters are examined with a theoretical analysis. Finally, simulations of the selected converters are performed and their advantages and disadvantages are clearly revealed.

2. CLASSICAL AND MODIFIED QUADRATIC BOOST DC-DC CONVERTERS

2.1. Classical Quadratic Boost Converter (CQBC)

Various DC-DC boost converter structures, isolated and non-isolated, are used to obtain high voltage gain in different areas, including renewable energy applications. Topologies such as bridge, flyback and forward are among the frequently preferred types of these converters. However, the use of transformers in these topologies causes disadvantages such as high volume, loss and cost. For the reasons mentioned, the development of converters aimed at obtaining high voltage gain has triggered the search for more economical and efficient solutions, especially in this area. In this direction, DC-DC converters providing high voltage gain have gained popularity and found a wide area of use. One of these converters is CQBC, which can provide higher gain and efficiency than more than one series-connected conventional boost DC-DC structures at the same duty cycle. This type of converters gets its name from the mathematical increasing of its gain with a two-stage structure. Its advantage with compared the conventional boost DC-DC converters is that it can obtain a higher output voltage with the same input voltage and duty cycle (Tattiwong and Bunlaksananusorn, 2014). The circuit topology of CQBC is given in Figure 1.

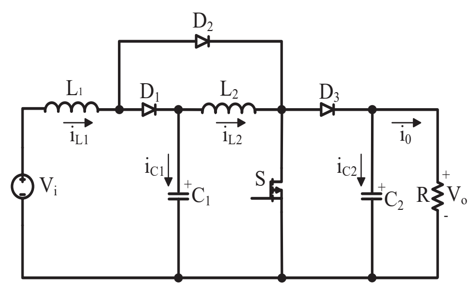

Figure 1. *The circuit topology of the CQBC*

In the CQBC circuit schema in Figure 1, V_i is called the input voltage, V_O is called the output voltage. C_1 and C_2 represent the filter capacitors; L_1 and L_2 represent the filter inductances. D_1, D_2 and D_3 are semiconductor power diodes; S is the semiconductor power switch. In the theoretical analysis of the circuit, it is assumed that the semiconductor power elements are ideal and that the voltage and current values of the inductances and capacitors are large enough to be constant. Assuming that the converter operates in continuous conduction mode (CCM), two operating modes can be examined in a switching period according to the on-state and off-state of the semiconductor power switch. The circuit schemas of the operating modes of the CQBC are given in Figure 2.

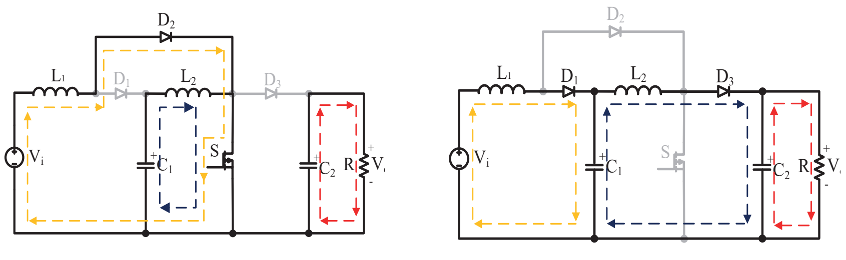

(a) **(b)**

Figure 2. *Equivalent circuit schemas of the operating modes of CQBC* ***(a)*** *The switch is on-state.* ***(b)*** *The switch is off-state.*

Mode 1: As seen in Figure 2 (a), in this operating mode, the S switch is at on-state and the input voltage source transfers energy directly to the L_1 inductance via the switch. Simultaneously, the C_1 capacitor is discharged via the switch and transfers its energy to the L_2 inductance. Thus, both the L_1 and L_2 inductances store energy and the current of the inductances reaches their maximum values at the end of this mode. In this mode, the D_1 and D_3 diodes are at off-state by being reverse-biased. On the output side, the C_2 capacitor continues to supply the load and the output voltage are constant. This mode is the stage where energy accumulation occurs in the inductances to be used in the next mode. The characteristic equations obtained using Kirchoff's voltage and current laws for this mode are given below:

$$V_{L_1} = V_i \quad (1)$$

$$V_{L_2} = V_{C_1} \quad (2)$$

$$I_{C_1} = -I_{L_2} \quad (3)$$

$$I_{C_2} = -I_O \quad (4)$$

Mode 2: As seen in Figure 2 (b), when the S switch is off-state, the energy transfer of the inductances begins. In this case, a portion of the energy in the L_1 is transferred to the C_1 capacitor, and the remaining portion is transferred to the output capacitor C_2 and the load through the L_2 inductance and the D_1 and D_3 diodes. At this mode, D_1 and D_3 diodes are on-state and D_2 diode is off-state. Concequently, the output voltage reaches a higher level with the contribution of both the L_1 and L_2 inductances. The characteristic equations obtained using Kirchoff's voltage and current laws for this mode are given below:

$$V_{L_1} = V_i - V_{C_1} \tag{5}$$

$$V_{L_2} = V_{C_1} - V_{C_2} \tag{6}$$

$$I_{C_1} = I_{L_1} - I_{L_2} \tag{7}$$

$$I_{C_2} = I_{L_2} - I_O \tag{8}$$

Using the voltage equations of the inductances L_1 and L_2, the gain equation of the converter can be obtained as follow:

$$M = \frac{V_O}{V_i} = \frac{1}{(1-D)^2} \tag{9}$$

2.2. Modified Quadratic Boost Converter (MQBC)

After CQBC is introduced to the literature, studies are conducted on improved and modified types of this converter. Unlike CQBCs, MQBCs are generally converters with increased element count and increased gain. The circuit topology of MQBC, one of the most up-to-date of these converters, designed by Naresh et al. (2025), is presented in Figure 3. In the presented converter, V_i is the input voltage, L_1 and L_2 represent inductances. There are two semiconductor power switches in the circuit, S_1 and S_2. In addition; D_1, D_2, D_o represent semiconductor power diodes in the converter, C_1, C_2, C_o represent capacitors. In the theoretical analysis of the circuit, it is assumed that the semiconductor power elements are ideal and the voltage and current values of the inductances and capacitors are large enough to be constant. Assuming that the converter operates in CCM, two operating modes can be examined in a switching period according to the on-state and off-state of the semiconductor power switches. The circuit schemas of the operating modes of the MQBC are given in Figure 4. The advantages of this converter include wide-range second-order voltage gain, constant input current characteristics, and reduced electrical stress.

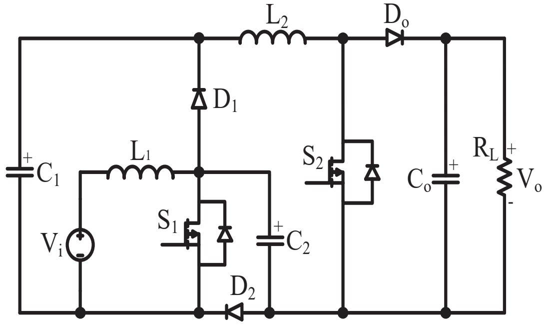

Figure 3. *The circuit topology of the MQBC*

Mode 1: In this mode, the control signals are given to S_1 and S_2, and so, the switches turn on. The equivalent circuit schema of this mode is shown in Figure 4 (a). In the circuit, the L_1 inductance is energized with the input voltage V_i. Thus, its current gradually increases and reaches its maximum level. At the same time, the L_2 inductance is energized by C_1 and C_2, and the its current increases linearly. In this operating mode, all diodes in the circuit are at off-state. The output capacitor Co feeds the output and provides the necessary energy to the load. The characteristic equations obtained using Kirchoff's voltage and current laws for this mode are given below:

$$V_{L_1} = V_i \tag{10}$$

$$V_{L_2} = V_{C_1} + V_{C_2} \tag{11}$$

$$I_{C_1} = I_{C_2} = -I_{L_2} \tag{12}$$

$$I_{C_O} = I_O \tag{13}$$

Mode 2: In this mode, the control signals of the semiconductor power switches are removed. The equivalent circuit schema and current paths of this mode are as shown in Figure 4 (b). All diodes in the circuit are forward-biased and they are at on-state. In this mode, the input voltage and the L_1 inductance, which is energized in the previous operating mode, charge the capacitors C_1 and C_2. At the same time, the energy of the input voltage V_i, L_1 and L_2 inductances are transferred to the output capacitor C_o and the load resistance RL. Thus, the energy required by the load continues to be provided. The characteristic equations obtained using Kirchoff's voltage and current laws for this mode are given below:

$$V_{L_1} = V_i - V_{C_1} = V_i - V_{C_2} \tag{14}$$

$$V_{L_2} = V_{C_1} - V_O \tag{15}$$

$$I_{C_1} = I_{C_2} = \frac{I_{L_1} - I_{L_2}}{2} \tag{16}$$

$$I_{C_O} = I_{L_2} - I_O \tag{17}$$

Using the voltage equations of the inductances L_1 and L_2, the gain equation of the converter can be obtained as follow:

$$M = \frac{V_O}{V_i} = \frac{1+D}{(1-D)^2} \tag{18}$$

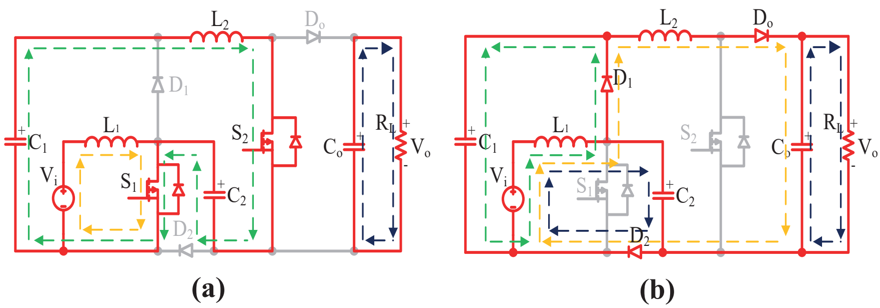

Figure 4. *Equivalent circuits of the operating modes of high gain MQBC* ***(a)*** *The switch is at on-state.* ***(b)*** *The switch is at off-state.*

3. SIMULATION RESULTS

In order to accurate of the theoretical analysis, the refered converters are simulated in the simulation programme. The simulation results presented are important in order to verify the performance of the circuit designs, to detect possible faults in advance and to evaluate the stability of the system. The simulation circuit schema of the CQBC is shown in Figure 5. The design parameters in the simulation are specified in Table 1. The simulation results are presented in Figures 6-9 for the evaluation of the circuit's operating analysis.

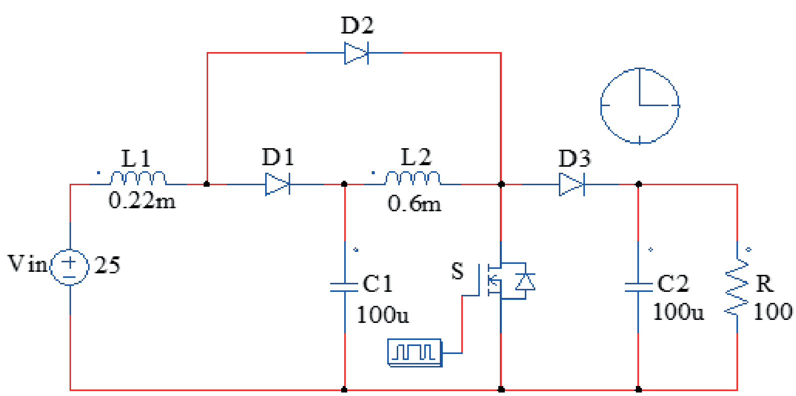

Figure 5. *The simulation circuit scheme of the CQBC*

Table 1. The simulation parameters in CQBC

Parameter	Symbol	Value
Input voltage	V_i	25 V
Output voltage	V_o	100 V
Swithing frequency	f	50 kHz
Output power	P_o	100 W
Inductances	L_1 / L_2	0,22 mH / 0,6 mH
Capacitors	C_1 , C_2	100 µF

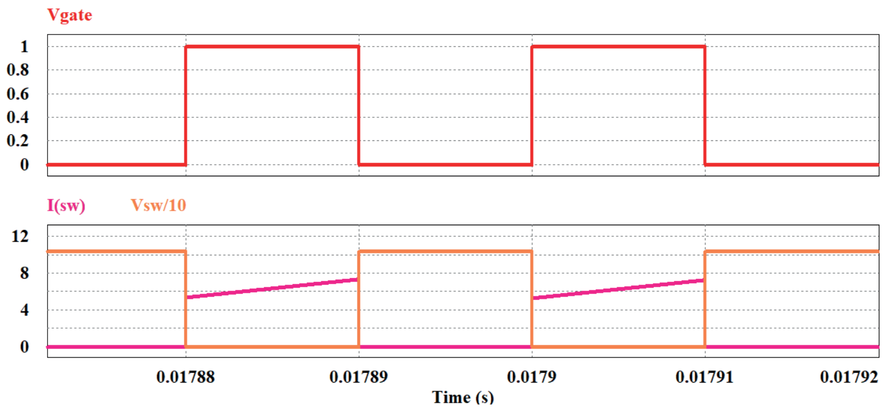

Figure 6. *The control signal, the current and voltage of the switch.*

The control signals, the current and voltage waveforms of the semiconductor power switch are given in Figure 6. As seen in the figure, the voltage to which the switch is exposed when it is in the off-state is at the same level as the output voltage such as in a conventional boost converter structure.

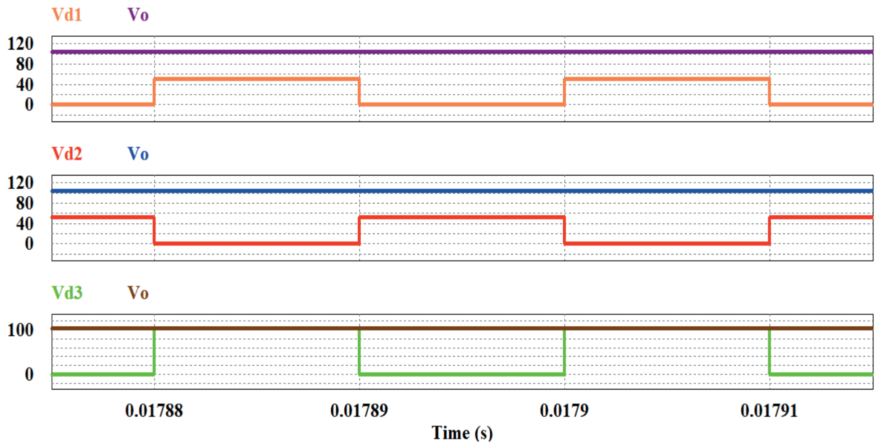

Figure 7. *The output voltage; the voltages of D_1, D_2 and D_3 diodes, respectively.*

In Figure 7, the voltage waveforms of the semiconductor power diodes D_1, D_2 and D_3 are given respectively. They are also compared with the output voltage. The voltage that the D_3 diode is exposed in the off-state is equal to the output voltage. In addition, the voltage to which the D_1 and D_2 diodes are exposed is half of the output voltage. This case is an advantage for the converter.

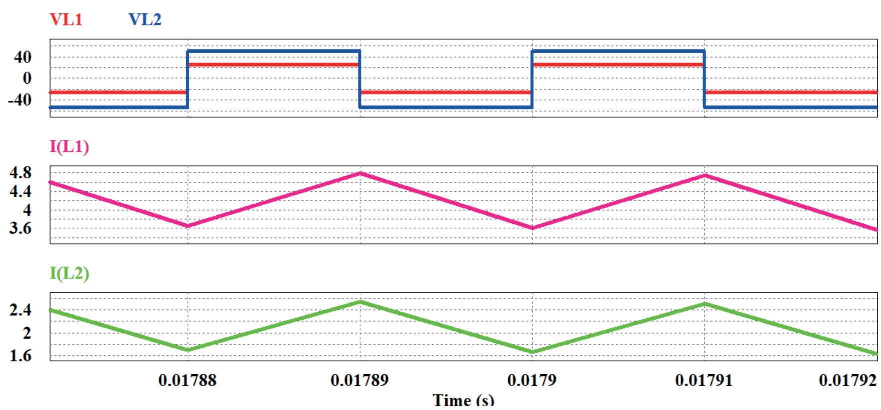

Figure 8. *The current and voltage of the L_1 and L_2 inductances, respectively.*

The voltage and current waveforms of the L_1 and L_2 inductances are given in Figure 8, respectively. As can be seen from the simulation results, when the switch is on-state, the currents of the L_1 and L_2 inductances increase and reach their maximum values. When the switch is off-state, the inductances are exposed to negative voltage and their currents decrease. Thus, the energy received and given by the inductances in the steady state are equal.

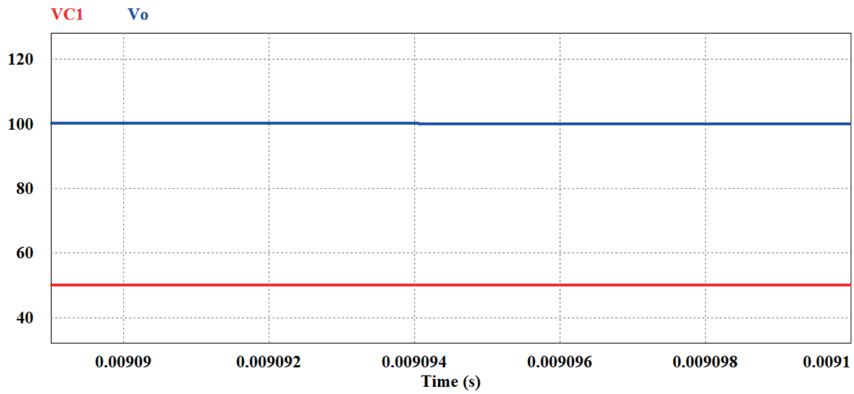

Figure 9. *The output voltage and the voltage of C_1 capacitor.*

In Figure 9, the output voltage and voltage waveforms of capacitor C_1 are given. The voltage of capacitor C_2 is also the output voltage. As can be seen from the figure, the voltage which capacitor C_1 is exposed is equal to half of the output voltage.

Another study examined in this chapter is the study conducted by Naresh et al. (2025), which is one of the MQBC circuits. The simulation circuit schema of this study is given in Figure 10. The parameters of the elements used in the simulation are listed in Table 2. The simulation results are presented in Figures 11-14.

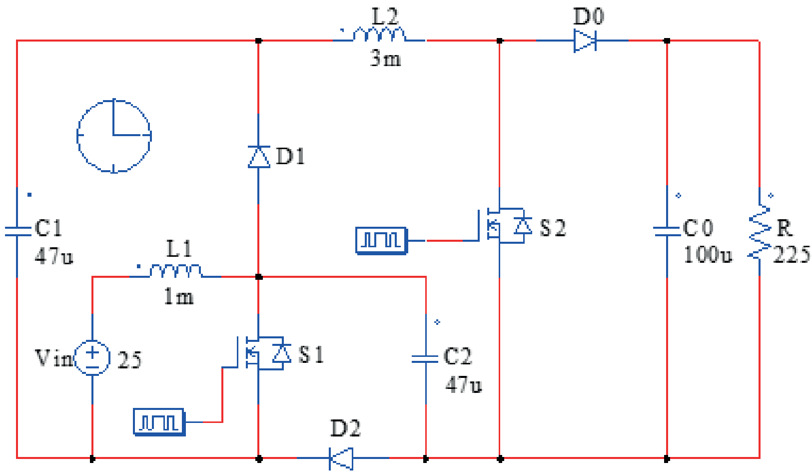

Figure 10. *The simulation circuit scheme of the MQBC*

Table 2. *The simuşation parameters in MQBC*

Parameter	Symbol	Value
Input voltage	V_i	25 V
Output voltage	V_o	150 V
Swithing frequency	f	50 kHz
Output power	P_o	100 W
Inductances	L_1, L_2	1 mH, 3 mH
Capacitors	C_1 ,C_2, C_o	47 µF, 47 µF, 100 µF

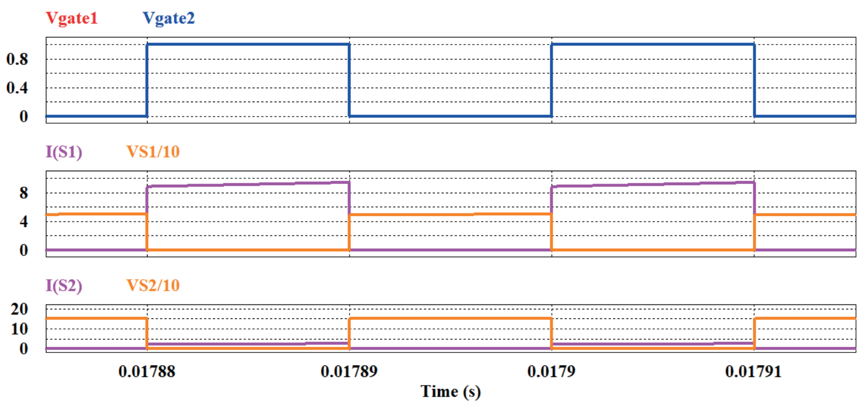

Figure 11. *The control signals of the switches; the waveforms of the current and voltage of the S_1 and S_2 swithces, respectively.*

Figure 11 shows the control signals of semiconductor power switches S_1 and S_2 and the current and voltage waveforms of the switches. Both switches are simultaneously turned on and off. As seen in the figure, the voltage that switch S_1 is exposed a less voltage than half of the output voltage, while the voltage that switch S_2 is exposed to the output voltage in the off-state. This is a significant advantage for switch S_1. At the same time, it is seen that the current stress of the switch S_1 is considerably higher than the current stress of the switch S_2. In this case, it provides a significant advantage in terms of reducing conduction losses.

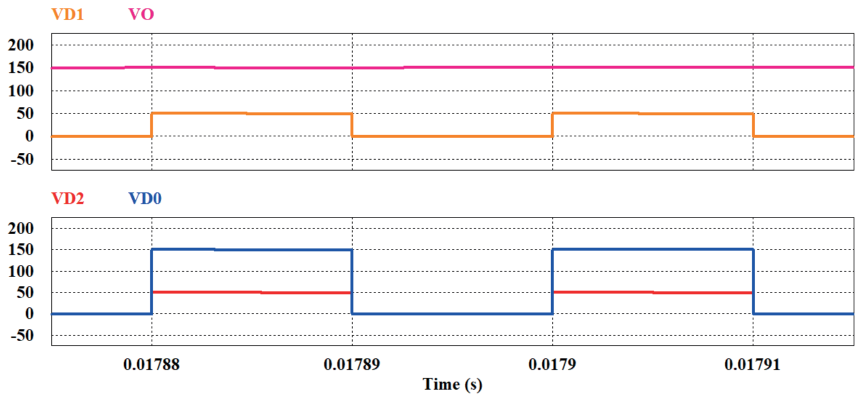

Figure 12. *The output voltage; the voltages of D_1, D_2 and D_O diodes, respectively.*

In Figure 12, the output voltage and voltage waveforms of the semiconductor power diodes D_1, D_2 and D_o are given. The voltage that the D_o diode is exposed is equal to output voltage in the off-state. In addition, it is seen that the voltage that which the D_1 and D_2 diodes are exposed is less than half of the output voltage.

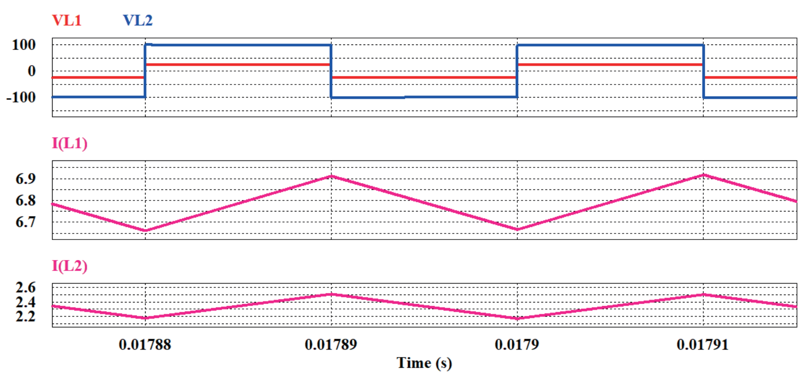

Figure 13. *The current and voltage of the L_1 and L_2 inductances, respectively.*

The voltage and current waveforms of the L_1 and L_2 inductances are given in Figure 13, respectively. As can be seen from the simulation results, the currents of the L_1 and L_2 inductances increase and reach their maximum values when the switches are at on-state. When the switches are at off-state, the inductances are exposed to negative voltage and their currents decrease. Thus, the energy received and given by the inductances are equal to each other in the steady state.

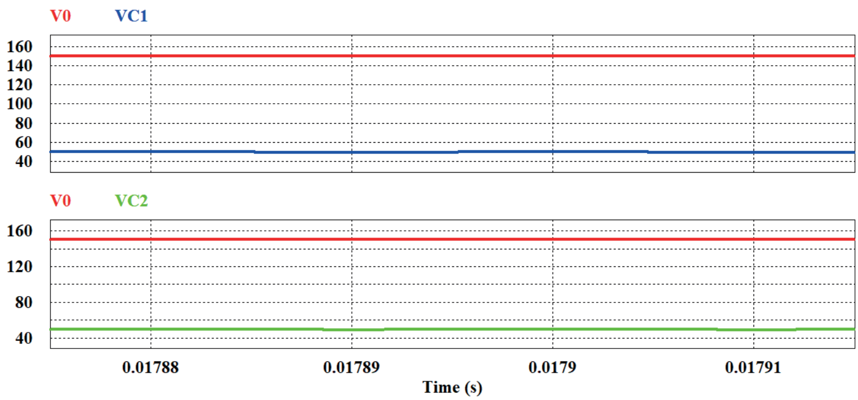

Figure 14. *The waveforms of the output voltage; the voltages of C_1 and C_2 capacitors, respectively.*

In Figure 14, the output voltage and the voltage of the capacitors in the circuit are given. These voltage waveforms are compared with the output voltage. It is shown that the voltages that capacitors C_1 and C_2 are exposed are less than half of the output voltage.

4. CONCLUSION

In this chapter, a study is conducted on the examination of quadratic boost converters that provide higher voltage gain than conventional boost converters. In this context, CQBC and MQBC in the literature are analyzed theoretically and compared with simulation results. Unlike the conventional boost converter, CQBC provides a gain of 4 times the input voltage at 50% duty cycle. The circuit topology consists of two inductors, three diodes, two capacitors and a semiconductor power switch. While the main power elements in the converter are exposed to the output voltage, the additional elements, the diodes, are exposed to a lower voltage than the output voltage. Another examined and modified structure, MQBC, provides a gain of 6 times the input voltage at 50% duty cycle, unlike the conventional boost converter. The circuit topology consists of two inductors, three diodes, three capacitors and two semiconductor power switches. While the main power elements in the converter are exposed to the output voltage, the additional elements, the diodes and the switch, are exposed to a lower voltage than the output voltage. Although this converter provides a higher voltage gain than CQBC, the converter has an extra switch and a capacitor, which is a disadvantage in terms of cost and losses.

REFERENCES

Haegel, N. M. and Kurtz, S. R. (2021) "Global Progress Toward Renewable Electricity: Tracking the Role of Solar", ***IEEE Journal of Photovoltaics***, 11(6), 1335-1342.

Lakshmi, M. and Hemamalini, S. (2018) "Nonisolated High Gain DC–DC Converter for DC Microgrids", ***IEEE Transactions on Industrial Electronics***, 65(2), 1205-1212.

Lee, S. W. and Do, H. L. (2019) "Quadratic Boost DC–DC Converter with High Voltage Gain and Reduced Voltage Stresses", ***IEEE Transactions on Power Electronics***, 34(3), 2397-2404.

Ogunrinde, O., Shittu, E. and Dhanda, K. K. (2018) "Investing in Renewable Energy: Reconciling Regional Policy with Renewable Energy Growth", ***IEEE Engineering Management Review***, 46(4), 103-111.

Qazı, A., Hussaın, F., Dhanda, K. K., Rahim, N., Hardaker, G., Alghazzawı, D., Shaban, K. and Haruna, K. (2019) "Towards Sustainable Energy: A Systematic Review of Renewable Energy Sources, Technologies, and Public Opinions", ***IEEE Access***, *7*, 63837- 63851.

Singh, K. A., Prajapati, A. and Chaudhary, K., (2022) "High-Gain Compact Interleaved Boost Converter With Reduced Voltage Stress for PV Application", ***IEEE Journal of Emerging and Selected Topics in Power Electronics***, 10(4), 4763-4770.

Yang, L. S., Liang, T. J. and Chen J. F. (2009) "Transformerless DC–DC Converters with High Step-Up Voltage Gain", ***IEEE Transactions on Industrial Electronics***, 56(8), 3144-3152.

Yang, J., Li, R., Ma, K. and Xu, J. (2023) "A Distributed Multimode Control Strategy for the Cascaded DC–DC Converter Applied to MVAC Grid-Tied PV System", ***IEEE Transactions on Industrial Electronics***, 70(3), 2617-2627.

Tattiwong, K. and Bunlaksananusorn, C. (2014) "Analysis Design and Experimental Verification of a Quadratic Boost Converter", ***TENCON 2014 - 2014 IEEE Region 10 Conference, Bangkok, Thailand,*** pp. 1-6.

Naresh, S. V. K., Li, Shareef, H., Kumar, B. and Peddapati, S. (2025) "Family of Capacitor–Diode Network Extended High Gain Quadratic Boost Converters for Microgrid Applications", ***IEEE Transactions on Power Electronics***, 40(1), 1418-1430.

CHAPTER 2

ELECTRIC VEHICLE CHARGING STATIONS AND HARMONIC PROBLEM

Ömer Ali KARAMAN[1],
Selahattin Barış ÇELEBİ[2],
Gökhan ÖZTÜRK[3]

1 Batman University Technical Sciences Vocational School, Batman/Türkiye, ORCID: 0000-0003-1640-861X, mail: omerralikar@gmail.com
2 Visiting Research Fellow: Department of Computer Science, University of Warwick, Coventry, UK, ORCID: 0000-0002-6235-9348, mail: sbariscelebi@gmail.com
3 Batman University Technical Sciences Vocational School, Batman/Türkiye, ORCID: 0000-0002-2780-6966, mail: ozturk.gkhn23@gmail.com

1. Introduction

In the context of the ongoing battle against global climate change, initiatives aimed at mitigating CO2 emissions have experienced an upsurge in activity (Oner et al., 2022). The proliferation of electric transportation networks is pivotal to these initiatives. Türkiye is likewise engaged in research endeavours aligned with international environmental objectives (Ozturk et al., 2021). According to the International Energy Agency (IEA), in its World Energy View 2017 (World Energy Outlook 2017) report, it is projected that nearly 40% of the automotive fleet will consist of electric vehicles (EVs) by the year 2040. With the implementation of regulatory measures in European nations, it is anticipated that carbon dioxide emissions will decline to approximately 59 grams per kilometer by the year 2030. Otherwise, it is expected that a penalty of 95 euros for each excess gram per vehicle. In order not to receive serious penalties in Europe, all brands are making efforts to produce electric cars with panic emissions. Figure 1 shows the amount of electricity vehicles of some countries between 2012-2024. As can be seen from the figure, the number of electric vehicles from year to year has increased exponentially (Global EV outlook, 2024).

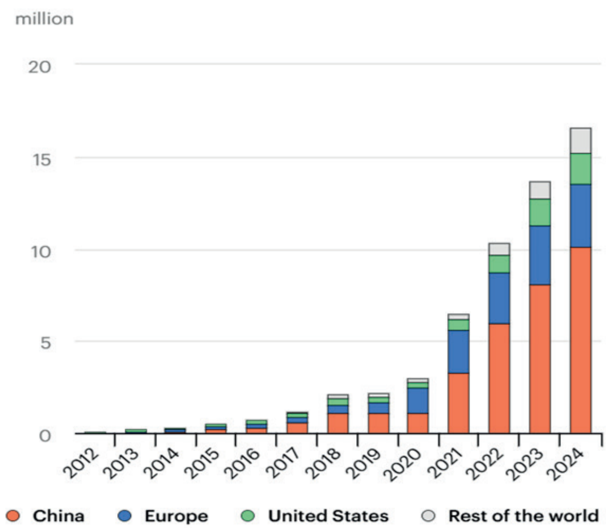

Figure 1. *Number of electric vehicles by years*

This increasing popularity of electric vehicles leads to a radical transformation in the transportation sector throughout the world. This transformation also causes significant changes in electrical infrastructure.

2. TYPES OF ELECTRIC VEHICLE CHARGING STATIONS

With the proliferation of electric vehicles, a multitude of charging stations has been designed to cater to diverse requirements and operational contexts. These stations are differentiated by their charging duration, power output, and technological characteristics. The main categories of the electric vehicle charging stations specified in Figure 2 are presented.

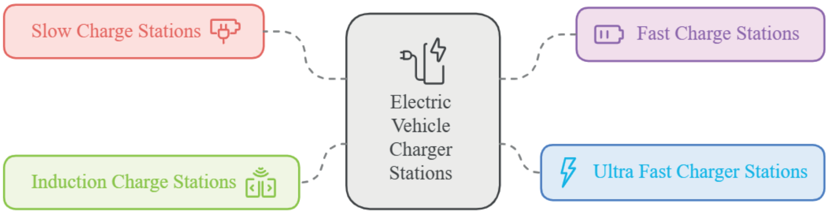

***Figure 2** Types of Electric Vehicle Charging Stations*

2.1. Slow Charging Stations (Type 1 and Type 2)

Slow charging stations are predominantly favored by individual users in residential and occupational settings due to their cost-effectiveness and ease of accessibility. These stations:

- **Type 1:** employs a single-phase system and is frequently encountered in North America and Japan. The power capacity is approximately 3.7 kW and necessitates a duration of 6-8 hours for the complete charging of an electric vehicle.

- **Type 2:** adheres to European standards and is compatible with both single-phase and three-phase systems. The power capacity ranges from 7-22 kW and requires a time frame of 4-6 hours to achieve full charging of an electric vehicle.

Slow charging has become a widespread choice because it is economic as well as compatible with the existing electrical infrastructure (Kumar et al., 2022).

2.2. Fast Charging Stations (DC Fast Charging)

Fast charging stations possess the capability to replenish the energy storage systems of electric vehicles within a brief duration due to their elevated power output. These stations:

• Typically exhibit a power capacity ranging from 60 to 150 kW.

• Can achieve an 80% state of charge for the battery within an average timeframe of 30 to 60 minutes.

• Are extensively located in commercial districts, shopping centers, and rest areas along highways. Fast charging stations constitute a critical infrastructural solution that enhances efficiency, particularly for individuals engaged in intercity travel (Ullah et al., 2023).

2.3. Ultra-Fast Charging Stations

Ultra-fast charging stations represent a significant advancement in the realm of electric vehicle technology, specifically engineered for high-performance vehicles. These stations:

• Possess high power capacities ranging from 103 to 250 kW.

• Have the capability to charge electric vehicles within a brief duration of approximately 30 minutes.

• Have been meticulously optimized for electric vehicles equipped with long-range and high-capacity batteries. These charging stations effectively alleviate the charging apprehensions of electric vehicle users by offering an experience that is comparable to that of internal combustion engine vehicles in terms of functionality (Valedsaravi et al., 2022).

2.4. Induction Charging Stations

Induction charging stations facilitate energy transfer without necessitating a physical connection, employing advanced wireless charging technology. These stations:

• Operate through specialized platforms installed beneath the vehicles.

• Exhibit considerable practicality due to their requirement for minimal physical interaction.

• Have been developed in both static forms (charging while parked) and dynamic forms (charging in motion) as induction systems. Induction charging systems, which are regarded as the prospective charging technology of the future, possess the capacity to enhance user experience and expedite the widespread adoption of electric vehicles (Guo et al., 2023).

3. WORKING PRINCIPLE OF ELECTRIC VEHICLE CHARGING STATIONS

Charging stations serve to regulate and manage the flow of electric current in order to supply energy to the vehicle's battery. The operational procedure unfolds as follows: The electricity drawn from the electrical grid to energize the charging station is subjected to processing by the station's power conversion systems. Through the utilization of AC-DC converters (rectifiers) or DC-DC converters, the electricity sourced from the grid is transformed into the appropriate direct current (DC) required by the vehicle's battery. Throughout the charging operation, the condition of the battery (including voltage, temperature, charging status, etc.) is systematically monitored. During the charging phase, the control mechanisms are engaged to avert scenarios of battery overheating or excessive charging. Upon the battery achieving the predetermined charging level, the charging station autonomously ceases the charging process.

Traditional charging methodologies encompass constant current (CC), constant voltage (CV), constant power, and leakage current techniques. In recent advancements, more sophisticated charging technologies have been developed to enable expedited battery charging methodologies, including constant current- constant voltage and impact as well as negative impact charging. This research specifically examines constant current (CC), constant voltage (CV), delta current/delta voltage (DI/DT-DV/DT), and controlled continuous current and continuous voltage (CC-CV) in the context of rapid charging.

3.1. Constant Current (CC)

Constant current (CC) charging is the simplest method in which a low - level current is given to a depleted battery. Typically, the current is set to 10 %of the maximum nominal capacity of the current. This charging approach is especially effective for nickel-cadmium and nickel-metal hydride battles. However, if the battery is excessive charging, it can cause problems such as gas and overheating. Similarly, illegal current charging involves the application of a small current to prevent the self -discharge of the battery. This method is generally used in emergency power backup systems and is compatible with lead-acid batteries (Kusdogan, 2017).

3.2. Constant Voltage (CV)

The battery undergoes a variation in voltage while maintaining a constant current. The magnitude of the current is typically established at 10% of the battery's rated capacity. The charging procedure persists until the battery voltage attains the predetermined threshold. Nickel-metal hydride (Ni-MH) and nickel-cadmium (Ni-CD) batteries utilize the constant current (CC) methodology for charging. This approach is frequently employed to energize the battery by applying a stable voltage across the terminals. During the initial phase of charging, the magnitude of the charging current is elevated. Once the battery voltage reaches the voltage calibration limit set by the charger, the charging current diminishes. This form of regulation is implemented in scenarios necessitating prolonged charging durations to achieve complete charge. Due to the extended charging time required, this may lead to increased temperatures and a reduction in the operational lifespan of the battery (Banguero et al., 2018).

3.3. Pulse Charging

The pulsed charging (PC) methodology encompasses the systematic application of impact currents to the battery at predetermined intervals. Within this framework, the batteries are intermittently discharged followed by subsequent recharging, a process referred to as equalization charging. This methodological approach aids in the stabilization of battery voltage over an extended duration. When implementing this technique, it is imperative to take into account various parameters such as charging frequency, impact peak, and impact duration, as these factors significantly influence both the battery's capacity and the overall duration of the charging process. A notable advantage of impact charging lies in its capacity to mitigate polarization, thereby contributing to the prevention of undesirable increases in battery temperature (Hua & Syue, 2010). Conversely, the intricate nature of this methodology may be perceived as a drawback.

3.4. Reflex charging or negative pulse charging (NPC)

Reflex charging, colloquially referred to as negative pulse charging (NPC), signifies an advancement in accordance with the PC methodology. The notion of NPC was first articulated in 1971 through the patents filed by W. Burkett, J. Bigbee, and subsequently by W. Burkett and R. Jackson (Nasser, 2017). The NPC methodology encompasses the regulation of a specific sequence of charging which integrates a positive charging effect, an interval devoid of charging activity, and a discharge effect frequently termed "burping." This methodology mitigates the thermal escalation of the battery by proficiently curtailing polarization (Li et al., 2009). Nevertheless, a potential drawback is its propensity to induce a reduction in charging efficiency (James et al., 2006).

3.5. Trick or Taper-Current-Tc

Trick charging, also referred to as taper current (TC) charging, encompasses the provision of a low rate of continuous constant current (CC) at a diminished rate relevant to the battery. This methodology is predominantly engineered to counteract the self-discharge phenomenon intrinsic to the battery (Xu at al., 2024). By employing an exceedingly minimal charging current, it is capable of effectively replenishing this specialized battery to a full capacity of 100%. This technique is frequently utilized in applications involving anthem, ignition, or starter (SLI) batteries. Nonetheless, it is not advisable for use with sensitive batteries, as they may incur damage due to excessive charging.

3.6. Float Charging-FC

Float charging (FC) entails a constant voltage (CV) charging mechanism that is adequate to facilitate the completion of battery charging or to maintain the battery at its maximum charge capacity. This particular methodology is especially advantageous for stationary batteries, notably those based on lead-acid technology. Conventional charging regulation techniques of this nature are incorporated into the commercially available inverters produced by companies such as Victron Energy and Sunny Island Solar Technology (Chuang et al., 2012).

3.7. Constant current and constant voltage (CC-CV) fast charging

The battery charger is the basis for filling the energy in electric car batteries. The current and voltage values are adjusted according to the characteristics of the charging battery. A charger may affect the time, battery charging and battery performance (Gao et al., 2020). If the voltage and current of the DC power supply is too high, it destroys battery cells, so that excessive charge may occur in the battery and shorten its life. However, if the DC power supply is too low, the battery will not charge. One of the things that must be done to overcome these problems is to apply a method called a constant current-constant voltage (CC-CV) system when charging the battery. The constant current is applied at the beginning of the battery charging cycle. When the battery voltage reaches the maximum voltage value, the charging device switches to constant voltage (CV) charging mode and the battery continues to charge it in this mode until it is completely charging (Chen et al., 2020).

The CC-CV methodology represents an integration of constant current (CC) and constant voltage (CV) techniques. This charging approach is often referred to as a biphasic method due to its incorporation of two distinct processes. Prior to initiating the charging sequence, it is imperative to ascertain the current and voltage parameters of the charger. The operational principle underpinning the CC-CV charging methodology posits that the battery undergoes an initial phase of constant current charging until the maximum permissible voltage is attained. The initial phase is intentionally selected to facilitate the charging of the battery at elevated current levels, as this practice minimizes adverse effects on the battery, such as thermal generation, thereby enhancing safety and longevity. Subsequently, the process transitions to the constant voltage mode until the battery reaches full capacity. The CC-CV charging protocol is superior to solely employing either constant current or constant voltage charging methods.

The CC-CV methodology facilitates rapid charging while mitigating the risk of overcharging, rendering it applicable to a diverse array of battery types. Through the implementation of this technique, the battery is capable of attaining its maximum capacity. The Fuzzy Logic Controller employs variations in voltage and current as the input parameters, while utilizing battery voltage as the variable for charging. The voltage of the battery is anticipated to rise in correspondence with the specified charging voltage and current. By employing this approach, the battery will achieve full charge in accordance with its designated capacity, thus preventing the occurrence of overcharging (Muslimin et al., 2022).

The spread of electric vehicles has brought about the diversification of charging stations and a transformation that requires radical changes in electrical infrastructure. The operating principles of charging stations cause harmonics during energy transformation due to the use of AC-DC and DC-DC converters. These harmonics can adversely affect the quality of power in the network, lead to energy losses and disrupt system stability. In addition to slow, fast and ultra -fast charging stations, wireless charging systems can also produce different harmonic levels. Therefore, it is of great importance to control and reduce harmonics in order to develop the electric vehicle charging infrastructure in a sustainable and efficient way.

While electric vehicles demand large amounts of electrical energy to charge their batteries, harmonics are injected into the network at certain frequencies during this charging process. These harmonic components are shown in Figure 3.

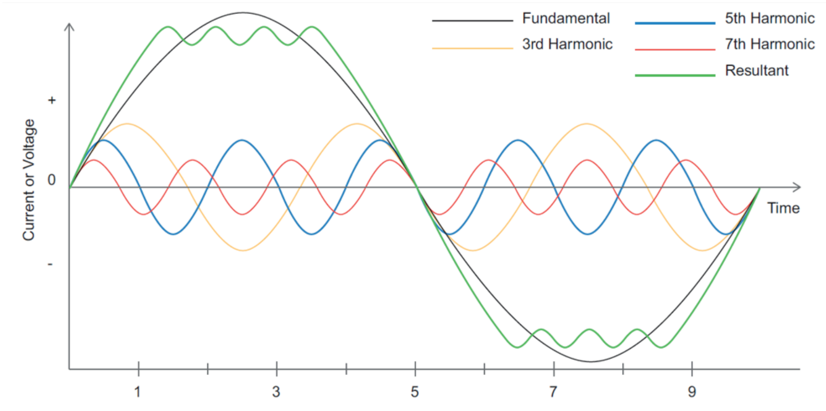

Figure 3 *Harmonic components*

Harmonics adversely affect the energy quality in the network by creating deviations from the ideal sinusoidal wave form of network electricity. In the following sections, the effects of harmonics caused by electric vehicle charging stations on the network and how these effects can be minimized.

4. HARMONICS

Electric vehicle charging infrastructures, power conversion apparatus, induction and resistance heating appliances, motor control systems, backup power systems, electronic ballast devices, solar energy systems, analog-to-digital and digital-to-analog converters, alongside the escalation in the utilization of non-linear electrical loads, as well as transmission and distribution networks, represent the predominant contributors to the degradation of electrical power quality. The tension harmonics engendered by current harmonics and current harmonics have emerged as a significant issue in numerous nations at present. To mitigate or eliminate these adverse effects, it is imperative that harmonics be attenuated within the network and harmonic compensation be implemented. Consequently, filters are employed to address harmonic issues in industrial contexts where non-linear loads are extensively prevalent. The metric that denotes the ratio of harmonics as a percentage is referred to as Total Harmonic Distortion (THB). THB serves as an indicator that reflects the degradation of current and voltage waveforms. In essence, THB represents the divergence of a periodic waveform from a sinusoidal waveform.

The THB, which is accepted according to the International IEEE 519-1992 standards, is 3 %for voltage and 5 %for current. In the harmonic proportions above these limit values, problems that may cause dangerous and major material damages for electrical systems may occur. THB is calculated as the ratio of the effective values of the harmonics to the effective value of the basic component. For current and voltage, THB expressions are given by equation (4.1) and equation (4.2).

$$THB_i = 100.\sqrt{\sum_{h\neq 1}\left(\frac{I_{sh}}{I_{s1}}\right)^2} \quad \textbf{(4.1)}$$

$$THB_V = 100.\sqrt{\sum_{h\neq 1}\left(\frac{V_{sh}}{V_{s1}}\right)^2} \quad \textbf{(4.2)}$$

Here I_{sh} is the current harmonics and I_{s1} the main component of the current, V_{sh} is the voltage harmonics and V_{s1} is the main component of the voltage.

Current and voltage harmonics cause excessive heating of transformers, burning of fuses, failure of circuit breakers to open and close, a decrease in the system's power factor and efficiency, a reduction in the lifespan of electrical devices, incorrect operation of measuring instruments, and an increase in measurement errors. Additionally, the harmonics generated in power systems lead to additional losses in components such as transformers, power transmission lines, motors, generators, capacitors, and others. In some cases, harmonics can also cause damage to power system components or lead to their malfunction.

4.1. Effects on Transformers

Harmonics are an important factor that increases losses and heating in the transformer. Current harmonics cause an increase in leakage flux and copper losses. Voltage harmonics cause increases in iron losses. As a result of these loss increases, additional warming occurs in the transformer. In addition, the harmonic components may cause resonance between transformer inductance and a load or circuit element connected to the transformer. All these losses are associated with frequency. With the increase in frequency, losses increase. Since the level of harmonic components increases, high -level harmonic components cause more losses than low -level harmonic components (Karaman et al., 2018). In general, iron losses that will occur in a magnetic core element are related to the voltage form to be applied to this element. If the harmonic voltage applied to a magnetic core element contains n harmonic components, the sudden value is referred to in mathematically equation (4.3).

$$V(t) = \sum_{n=1}^{N} V_n(t) \qquad \textbf{(4.3)}$$

The effective value of the voltage is given in the equation (4.4).

$$V = \sqrt{\sum_{n=1}^{N} {V_n}^2} \qquad \textbf{(4.4)}$$

Iron losses,

$$P_{Fe} \cong K_m V^2 = K_m \sum_{n=1}^{N} {V_n}^2 \qquad \textbf{(4.5)}$$

Expressed. Expressed. Voltage harmony ratio for nth of harmonic

$$\beta_n = \frac{V_n}{V_1} \quad \text{(n=2,3……N)} \qquad \textbf{(4.6)}$$

Iron losses can be written again by using the expression.

$$P_{Fe} \cong K_m {V_1}^2 (1 + \sum_{n=1}^{N} {\beta_n}^2) \qquad \textbf{(4.7)}$$

As seen in equation (4.7), in the presence of harmonics in the system, in addition to the losses caused by the fundamental component, losses caused by the harmonics also occur.

4.2. Effects on transmission lines

Harmonics create voltage drops on the transmission lines on the lines of losses and all elements connected to the system. The voltage drop formed by the nth Harmonic component of the current, is expressed;

$$|\Delta V_n| = |I_n||Z_n| \qquad \textbf{(4.8)}$$

The power loss of the current harmonics is shown in equation (4.9). The additional losses given here are.

$$P_k = \sum_{n=2}^{\infty} {I_n}^2 R_n \qquad \textbf{(4.9)}$$

In this equation nth shows harmonic component current, Rn shows omic resistance at the nth of the harmonic frequency.

4.3. Effects on motors and generators

Harmonics have a similar effect on motors and generators. Harmonics increase iron and copper losses in motors and generators and allow the heat to increase. Therefore, harmonic components cause a decrease in the efficiency and torque of rotating machines and make them operate more noisily. Each harmonic voltage (5th, 7th, 11th, ...) creates additional heat in the stator of the machine by inducting a harmonic current and stator winding. Thus, with the additions caused by the fundamental current component, the machine's temperature increases even further. The rise in motor temperature due to harmonics shortens the motor's lifespan (Hamidi et al., 2022).

5. HARMONIC REDUCTION METHODS

Nowadays, due to the increase in the use of non -linear loads in distribution systems, large amounts of deterioration have occurred in the form of current and voltage wave. There are several methods used in the literature to reduce or eliminate these harmonics. The most used methods; active power filters and passive power filters (Pattathurani et al., 2022).

5.1. Active Power Filters

Active filter is a general term. It consists of power switching devices and passive energy storage inductors and capacitors due to a group of power electronics circuits. The functions of these circuits may vary according to many different applications. Active Power Filters (APF) are generally used for controlling current harmonics in low and medium voltage power supplies or at high voltage distribution levels to control reactive power and voltage (Gali et al., 2017). The concept of APF was proposed by H.Sasaki and T.Cachida. In 1982, the APF, which consists of PWM inverter current source using 800 kVA GTO thyristor in the world for the first time in the world, was used to make harmonic compensation. In the following years, the developments in control strategies have led to rapid progress in APF techniques. Figure 4 shows the basic principle scheme of APF. In order to make the source current sinusoidal, the compensated current *ic* is injected into the source current *is* and the harmonic in the load current *iL* is removed

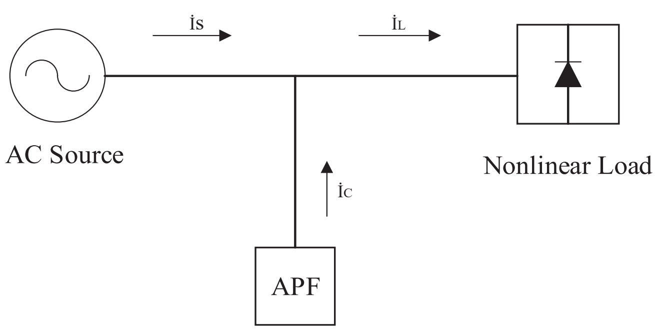

Figure 4 *APF's basic principle scheme*

APF structures are power electronic-based devices that switch the voltage or current generated on the capacitor or reactor in the AC network using power electronic switches, with the converter inside, and transmit the resulting voltage or current with different waveform structures to the grid. Although the investment cost of AGFs is more than passive filters, it is possible to respond to changing load conditions, that filtering performance is better, it is smaller in physical dimension, it is more flexible in applications, the ease of connection to the system and the quality of power quality problems. It emphasizes these structures (Karaman et al., 2020).

The ability of modern power transistors to be triggered at very high frequencies enables active power filters to suppress high-frequency current and voltage harmonics, perform reactive power compensation, eliminate imbalances in three-phase systems, and reduce neutral line currents. For this reason, active power filters are the most effective method for harmonic and reactive power compensation today (Herman et al., 2024).

APF selection for special applications is one of the most important tasks of application engineers and users. Because the application requirements are spread over a wide range of and large areas such as single phase or three -phase, three -wire or four -wire systems, current or voltage -based compensation. However, many active filter configurations can respond to the needs of individual users.

The most commonly used filters among APFs are Parallel Active Power Filters (PAPFs). These are connected in parallel to the load and inject currents into the grid that are equal in magnitude but opposite in phase to the harmonic currents, aiming to eliminate load current harmonics and perform reactive power compensation. In this way, the waveforms of the currents drawn from the source are made sinusoidal (Saihi & Berbaoui, 2023).

A PAPF; The inverter consists of a link capacitor, a connection inductance that connects the inverter to the network, a control unit that produces evolving switches and reference current. The inverter produces the compensation current. The task of the connection inductance used in the AC side of the driver prevents the switching parasites produced by the inverter. The control unit generates switching signals for the inverter. PAPF is divided into two parts according to the inverter structure. These are voltage-based PAPF and current-based PAPF. In parallel active power filters caused by voltage, the capacitor is used as energy storage elements and coil is used in parallel active power filters of current -induced parallel active power filters. Figure 5 shows the general circuit structure of a voltage-based PAPF (Karaman et al., 2018).

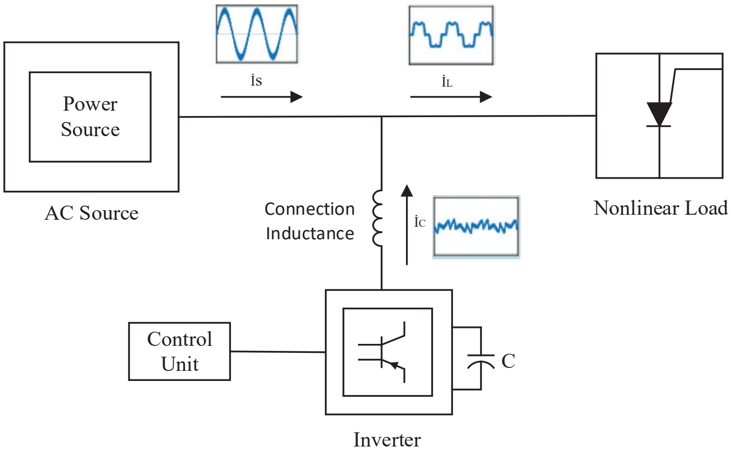

Figure 5 *Structure of voltage-based PAPF*

In Figure 6, a current based on PAPF is shown. The voltage-source inverter-based parallel active power filter is more commonly preferred in active power filter applications due to its higher efficiency, lower installation cost, and advantages such as ease of control compared to the current-source inverter-based parallel active power filter. On the other hand, current-sourced parallel active power filters are also used in APF structures because they directly switch the current, offering fast response times and features such as limiting the inductor current and providing short-circuit protection (Karaman et al., 2018).

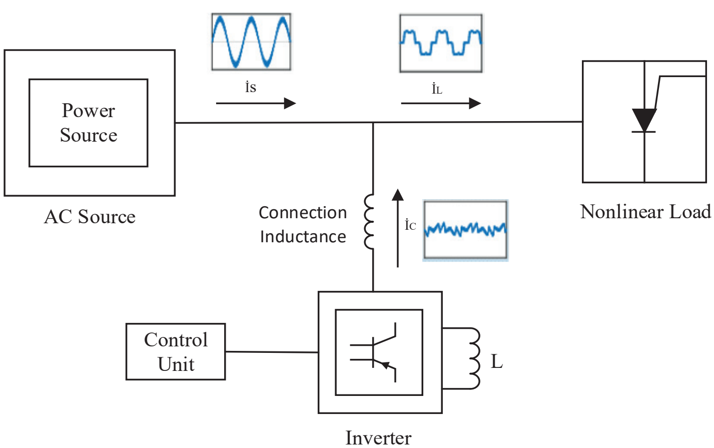

Figure 6 *Structure of current-based PAPF*

The most important component of the PAPF power circuit is the inverter. Two-level voltage-based inverters; It is widely used in PAPF power circuits due to its superiority such as easy application, cost of cost and ease of control. These inverters contain a capacitance in the DC link. Additionally, current-sourced inverters with inductance in the DC link are also used in PAPF power circuits, as they directly switch the current. A PAGF has both important duties. These are extraction of appropriate harmonic current references and production inverter switching signals for a compensation current in the opposite phase and equal amplitude by following this reference current ((Karaman et al., 2020).

5.2. Passive filters

Passive filters (PF) is consist of capacitor (C), an inductance (L) adjusted to the harmonic frequency to be filtered (L) and sometimes an omic resistance (R). This makes the filter configuration simple and easy to apply. Figure 7 shows various PF circuits. The task of these filters placed between the source and the load is to reduce or eliminate the effect of current or voltage harmonics in one or more frequency. For this purpose, passive power filters are specifically designed for the system to completely eliminate or reduce the effect of the most dominant harmonic component. Undesired harmonic components are diverted to the ground through a low-impedance path. Passive filters are frequently used in application due to their simple structure, low investment costs and ease of use (Anuar & Abdullah, 2022).

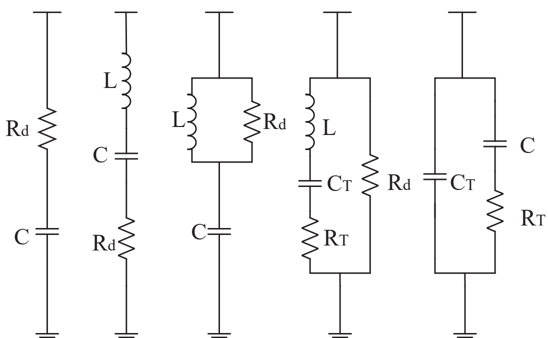

***Figure** 7 Various passive filter circuits*

PF has three main functions. The first is to prevent electromagnetic parasites produced by the switching source from reaching the power line and affecting other equipment. The second is to prevent the high frequency voltage in the power line from passing through the output of the power supply. Third is to develop the power factor and eliminate harmonics. The biggest drawback of passive filters in application is the resonance problem. In addition, these filters have a fixed compensation characteristic, as they are designed for a harmonic component to be filtered. This situation adversely affects filter performance in constant changing load applications (Dinis et al., 2024).

6. FUTURE PERSPECTIVE

Parallel active power filters, as advanced devices that actively detect and eliminate harmonics in the grid, hold significant potential for addressing harmonic issues. However, since grid conditions are dynamic, the effectiveness of these filters depends on their adaptability. At this point, artificial intelligence (AI) plays a crucial role in significantly enhancing the performance of parallel active power filters. Today, AI algorithms are a method frequently used in forecasting studies (Celebi, S.B., & Karaman, Ö.A., 2023). AI algorithms can monitor, analyse, and optimize operating conditions and harmonic distortions in real time, determining the most efficient filtering strategies tailored to the specific needs of each charging station. As a result, not only does the filtering process become more effective, but the overall efficiency of the grid also improves.

7. CONCLUSION

In this study, the effects of harmonics on electrical systems and the negative consequences of these effects on various devices, especially transformers, transmission lines, motors and generators were examined. In addition, operating principles and charging methods of electric vehicle charging stations are emphasized. The charging processes of electric vehicles vary according to the charging methods used and each method offers different advantages and disadvantages. Methods such as constant current, constant voltage, impact charging, and CC-CV charging are critical to extend the battery life and provide efficient charging. The effects of harmonics on electrical devices are spread to a wide range. In transformers, it has been observed that harmonics lead to overheating by increasing losses and decreasing system efficiency. The effects on the transmission lines are manifested as voltage decreases and the increase of loss forces. Motors and generators may face negative effects such as overheating and mechanical losses, especially due to harmonic currents. This not only reduces the efficiency of the devices, but also shortens their lives. The operating principles of electric vehicle charging stations play a critical role for the efficient and safe charge of the batteries. Optimizing parameters such as accurate current, correct voltage of charger prevents the battery from overheating and excessive charging. However, fast charging technologies play an important role in rapidly increasing battery capacities but should be carefully managed to minimize side effects such as excessive charging and heating.

Finally, the methods developed to reduce harmonics are of great importance in terms of increasing the efficiency of modern power systems and minimizing energy losses. Active and passive power filters are one of the most widely used solutions to minimize the effects of harmonics. Active power filters provide high -efficiency filtering, while passive filters offer simpler and economical solutions. Both methods make significant contributions to eliminating the negative effects of harmonics on the system. In this context, filtering technologies and charging methods used to reduce the effects of harmonics contribute to the creation of a safe and efficient working environment for electric vehicles and other electrical device. In the future, the continuation of research on harmonic management and charging technologies will provide significant gains in terms of energy efficiency and device life.

REFERENCES

Anuar, M., & Abdullah, N. (2022). Dominant Harmonic Current Reduction using Passive Power Filter. *2022 IEEE International Conference on Power and Energy (PECon)*, 186-191.

Banguero, E., Correcher, A., Pérez-Navarro, Á., Morant, F., & Aristizabal, A. (2018). A review on battery charging and discharging control strategies: Application to renewable energy systems. Energies, 11(4), 1021.

Chen, G., Liu, Z., & Su, H. (2020). An optimal fast-charging strategy for lithium-ion batteries via an electrochemical–thermal model with intercalation-induced stresses and film growth. Energies, 13(9), 2388.

Chuang, Y.C.; Ke, Y.L.; Chuang, H.S.; Chang, S.Y. (2012). Battery float charge technique using parallel-loaded resonant converter for discontinuous conduction operation. IEEE Trans. Ind. Appl. 48, 1070–1078.

Çelebi, S. B., & Karaman, Ö. A. (2023). Multilayer LSTM Model for Wind Power Estimation in the Scada System. *European Journal of Technique (EJT)*, *13*(2), 116-122.

Diniș, C. M., Popa, G. N., Cunțan, C. D., & Iagăr, A. (2024). Aspects Regarding of Passive Filters Sustainability for Non-Linear Single-Phase Consumers. *Sustainability*, *16*(7), 2776.

Gao, J. Y., Yang, Y. F., Zhang, X. K., Li, S. L., Hu, P., & Wang, J. S. (2020). A review on recent progress of thermionic cathode. Tungsten, 2, 289-300.

Gali, V., Gupta, N., & Gupta, R. (2017). Mitigaiton of Power Quality Problems Using Shunt Active Power Filters: A Comprehensive Review. 12th IEEE Conference on Industrial Electronics and Applications (ICIEA) (s. 1100-1105). Siem Reap, Cambodia: IEEE.

Global EV Outlook, (2024). (Accessed: 10 December 2024). https://www.iea.org/data-and-statistics/data-product/global-ev-outlook-2024#.

Guo, J., He, J., & Zhang, Y. (2023). The development of wireless charging technology in the electric vehicle. Highlights in Science, Engineering and Technology, 43, 1-10.

Hamidi, M., Adelpour, M., & Hamzeh, M. (2022). Prediction of Synchronous Generator Fatigue Life in Islanded Microgrids With Harmonic Loads. *IEEE Transactions on Energy Conversion*, 37, 2419-2427.

Herman, L., Knez, K., & Blažič, B. (2024). Design and Performance Evaluation of a Hybrid Active Power Filter Controller. *Energies*, *17*(11), 2492.

Hua, A.C.-C., & Syue, B.Z.-W. (2010). Charge and discharge characteristics of lead-acid battery and LiFePO4 battery. In Proceedings of the IEEE 2010 International Power Electronics Conference (IPEC), Sapporo, Japan, 21–24 June 2010; pp. 1478–1483.

James, M.; Grummett, J.; Rowan, M.; Newman, J. (2006). Application of pulse charging techniques to submarine lead-acid batteries. J. Power Sources 2006, 162, 878–883.

Karaman, Ö. A., Erken, F., & Cebeci, M. (2018). Decreasing harmonics via three phase parallel active power filter using online adaptive harmonic injection algorithm. *Tehnički vjesnik*, *25*(Supplement 1), 157-164.

Karaman, Ö. A., Gündoğdu, A., & Cebeci, M. (2020). Performing reactive power compensation of three-phase induction motor by using parallel active power filter. *International Advanced Researches and Engineering Journal*, *4*(3), 239-248.

Kumar K, J., Kumar, S., & VS, N. (2022). Standards for electric vehicle charging stations in India: A review. Energy Storage, 4(1), e261.

Kuşdoğan, Ş. (2017). Akıllı Şebekelere Elektrikli Araçların Entegrasyonu ve Taşıttan Şebekeye V2G Uygulamaları. V. Elektrik Tesisat Ulusal Kongre ve Sergisi, III. Güç ve Enerji Sistemleri Sempozyumu, Türkiye, 18 - 21 Ekim 2017.

Li, S., Zhang, C., Xie, S. (2009). Research on fast charge method for lead-acid electric vehicle batteries. In Proceedings of the IEEE International Workshop on Intelligent Systems and Applications ISA 2009, Wuhan, China, 23–24 May 2009; pp. 1–5.

Muslimin, S., Maulidda, R., Nawawi, M., Rahman, A., & Kurnia, P. M. (2023). The Method of Constant Current-Constant Voltage (CC–CV) for SECA Electric Car Battery Charging with Fuzzy Logic Controller. In 6th FIRST 2022 International Conference (FIRST-ESCSI-22) (pp. 14-23). Atlantis Press.

Nasser, K. (2017). Negative Pulse Charging: Myths and Facts. http://www.batterypoweronline.com/images/PDFs_articles_whitepaper_appros/powerdesigners.pdf.

Öner, C., Öztürk, G., & Tanyeri, B. (2022). Buji Ateşlemeli Bir Motorda Ultrasonik Yakıt Sistemi Kullanılmasının Egzoz Emisyonları Üzerindeki Etkisinin İncelenmesi. Afyon Kocatepe Üniversitesi Fen Ve Mühendislik Bilimleri Dergisi, 22(5), 1214-1224.

Öztürk, G., Tansu, M. N., & Umut, U. Z. (2021). Türkiye'de Hibrid Ve Elektrikli Araçlara Eğilimin Araştirilmasi. Journal On Mathematic, Engineering and Natural Sciences (EJONS), 5(20), 814-823.

Pattathurani, L. P., Dash, S. S., Dwibedi, R. K., Raj, M. D., Kannadasan, R., Savio, M. F., Alsharif, M. H., & Kim, J. H. (2022). Harmonics Minimisation in Non-Linear Grid System Using an Intelligent Hysteresis Current Controller Operated from a Solar Powered ZETA Converter. *Sustainability*, *14*(12), 7028.

Saihi, L., & Berbaoui, B. (2023). Mitigation of Low Voltage Electrical Network Pollution Using a Two-Level PAPF Controlled by the ANN-PQ Algorithm. *2023 International Conference on Electrical Engineering and Advanced Technology (ICEEAT)*, 1, 1-5.

Ullah, I., Liu, K., Layeb, S. B., Severino, A., & Jamal, A. (2023). Optimal Deployment of Electric Vehicles' Fast-Charging Stations. Journal of Advanced Transportation, 2023(1), 6103796.

Valedsaravi, S., El Aroudi, A., & Martínez-Salamero, L. (2022). Review of solid-state transformer applications on electric vehicle DC ultra-fast charging station. Energies, 15(15), 5602.

Xu, Y., Li, Y., Chen, Y., Zhou, W., Mai, R., & He, Z. (2024). A Multiple-Gain-Reconfigurable-Rectifier-Based IPT System for Battery Multistage Constant-Current High-Efficiency Wireless Charging. *IEEE Transactions on Power Electronics*, 39, 1853-1869.